Applied and Computational Mathematics
2022; 11(1): 18-30
http://www.sciencepublishinggroup.com/j/acm
doi: 10.11648/j.acm.20221101.12
ISSN: 2328-5605 (Print); ISSN: 2328-5613 (Online)

Bifurcations and Dynamical Behavior of 2D Coupled Chaotic Sine Maps

Yamina Soula[1,*], Abdel Kaddous Taha[2], Daniele Fournier-Prunaret[2], Nasr-Eddine Hamri[3]

[1]Department of Mathematics, Faculty of Sciences, University of Larbi Ben M'hidi, Oum el Bouaghi, Algeria
[2]Lattis-Insa, University of Toulouse, Toulouse, France
[3]Institute of Sciences and Technologie, University Center of Abd el Hafid Boussouf, Mila, Algeria

Email address:

h.soula@yahoo.fr (Y. Soula), taha@insa-toulouse.fr (A. K. Taha), daniele.fournie@insa-toulouse.fr (D. Fournier-Prunaret), n.hamri@centre-univ-mila.dz (Nasr-Eddine H.)
*Corresponding author

To cite this article:

Yamina Soula, Abdel Kaddous Taha, Daniele Fournier-Prunaret, Nasr-Eddine Hamri. Bifurcations and Dynamical Behavior of 2D Coupled Chaotic Sine Maps. *Applied and Computational Mathematics*. Vol. 11, No. 1, 2022, pp. 18-30. doi: 10.11648/j.acm.20221101.12

Received: January 14, 2022; **Accepted:** February 14, 2022; **Published:** February 18, 2022

Abstract: The main characteristics of a dynamical system are determined by the bifurcation theory. In particular, in this paper we examined the properties of the discrete dynamical system of a two coupled maps, i.e. the maps with an invariant unidimensional submanifold. The study of coupled chaotic systems shows rich and complex dynamic behaviors, particularly through structures of bifurcations or chaotic synchronization. A bifurcation is a qualitative change of the system behavior under the influence of control parameters. This change may correspond to the disppearance or appearance of new singularities or a change in the nature of singularities. We can define different kinds of bifurcations for fixed points and period two cycles as, saddle-node, period doubling, transcritical or pitchfork bifurcations. The study of the sequence of bifurcations permits to understand the mechanisms that lead to chaos. The phenomena of synchronization and antisynchronization in coupled chaotic systems is very important because its applications in several areas, such as secure communication or biology. In this paper, we study bifurcation properties of a two-dimensional coupled map T with three parameters. The first objective is to locate the bifurcation curves and their evolution in the parametric plane (a, b), when a third parameter c varies. The equations of some bifurcation curves are given analytically; cusp points and co-dimension two points on these bifurcation curves are determined. The second is related to the study of the chaotic synchronization and antisynchronization in the phase space (x, y).

Keywords: Two Dimensional Coupled Map, Bifurcation, Chaotic Synchronization and Antisynchronization

1. Introduction

Many studies have been devoted to coupled maps those last years. One of the major interest of their study is to understand their dynamical behavior and more particularly the way how synchronization phenomena can occur. Indeed, coupled systems may exhibit synchronized chaotic motion on an invariant subspace of the whole phase space [7, 8, 19]. The synchronization and antisynchronization of coupled chaotic oscillators have a variety of applications, particularly in connection with secure communication [5, 11] or biology. In this paper we consider a family of two-dimensional maps generated by the coupling of two one-dimensional maps including sine functions. We propose to extend the study proposed in [12] regarding the bifurcations and phenomena of synchronization and antisynchronization.

We consider a map of the following form:

$$X_{n+1} = T(X_n),\ X = (x, y) \in \mathbb{R}^2,\ \Lambda = (a, b, c) \in \mathbb{R}^3 \quad (1)$$

To understand the evolution of the dynamics of the map (1), we study the cycles of period k of T, that means k consecutive points $X_1, ...X_k$ satisfying $T(X_i) = X_{i+1}$, $i = 1, ...k-1$, $T(X_k) = X_1$, $X_i = T^k(X_i)$, $X_i \neq T^l(X_i)$, $i = 1, ...k$, $1 \leq l < k$, l, k integers.

In the case of a differentiable and of class $C^{(1)}$ one-dimensional map, a cycle possesses what is called a multiplier

S, which is defined as the product of the derivatives of the map at each point of the cycle. The cycle is said to be stable if $|S| < 1$, and unstable if $|S| > 1$.

In the case of a differentiable and of class $C^{(1)}$ two-dimensional map, a cycle has two multipliers S_1 and S_2, which are the eigenvalues of the jacobian matrix $DT^k(X)$ of the map T^k at one point of the cycle. The calculation of S_1 and S_2 is used to find the stability of the cycle:

1. a cycle is a saddle when S_1 and S_2 are real, $|S_1| < 1$, $|S_2| > 1$;
2. a cycle is a node when S_1 and S_2 are real, stable (or attracting) if $|S_i| < 1$ $(i = 1, 2)$, unstable (or repulsing) if $|S_i| > 1$ $(i = 1, 2)$.

In this paper, we do not consider the case of complex eigenvalues.

When $S_1 = +1$ or $S_2 = +1$, a saddle-node (fold) or transcritical or pitchfork bifurcation can occur:

1. saddle-node (or fold) bifurcation: two period k cycles appear at the bifurcation value, one is a node, the other is a saddle. We are more interested in the case of the appearance of a stable node.
2. transcritical bifurcation: the same number of period k cycles exists before and after the bifurcation value, but two period k cycles exchange their stability.
3. pitchfork bifurcation: one period k cycle changes its stability at the bifurcation value and gives birth to two symmetric period k cycles, which have the same stability as the original cycle before the bifurcation.

The equations permitting to obtain the curves corresponding to a bifurcation with $S_i = +1$, $i = 1$ or 2 are given below [3]. First, let us define $d = det(DT^k(X)) + 1$ and $N = trace(DT^k(X))$, and let the polynomyal of the Jacobian matrix $DT^k(X)$, given by $P(S) = S^2 - NS + d = 0$ be the characteristic of $\partial T^k(X)\partial X$. then we have:

$$\begin{cases} T^k(X) = X \\ d - N = 0 \end{cases} \tag{2}$$

When $S_1 = -1$ or $S_2 = -1$, a flip (period doubling) bifurcation occurs:

1. flip bifurcation: one period k cycle changes its stability at the bifurcation value and gives birth to one period $2k$ cycle, which has the same stability as the period k cycle before the bifurcation.

The equations permitting to obtain the curves corresponding to a flip bifurcation are the following [3]:

$$\begin{cases} T^k(X) = X \\ d + N = 0 \end{cases} \tag{3}$$

Such equations can be solved analytically or numerically using for instance a Newton-Raphson method.

In this paper is analyzed the dynamics of the map T, related to a coupling between one-dimensional maps f_a given below:

$$T : \begin{cases} x_{n+1} = F(x_n, y_n) = f_a(x_n) + (1 - c)bg(x_n,\ y_n), \\ y_{n+1} = G(x_n, y_n) = f_a(y_n) + bg(y_n,\ x_n), \end{cases} \tag{4}$$

Where x_n and y_n are state variables at a discrete time n, with $(x, y) \in [0, 1]^2$,

a is the control parameter of the uncoupled $1D$ map f_a:

$$f_a(x) = x + \frac{a}{2\pi}\sin(2\pi x), \tag{5}$$

b is a coupling parameter between the two subsystems, g is a coupling function of the form:

$$g(x, y) = \frac{1}{2\pi}\sin(2\pi(y - x)) \tag{6}$$

The third parameter c $(0 \leq c \leq 1)$ has been introduced in the map with the aim to better understand the dynamics of the map, more particularly the structure of bifurcations, when the coupling between the one-dimensional maps is symmetrical or not symmetrical. For a given value of c, bifurcation curves in the (a, b) parameter plane can be obtained using Eq. (2) and Eq. (3). A locus of bifurcations $(S_1 = +1)$ is a fold bifurcation curve denoted $\Lambda^j_{(k)_0}$, a locus of bifurcations $(S_1 = -1)$ is a flip bifurcation curve denoted Λ^j_k [14-18].

In this paper we also consider the following types of codimension two singularities:

1. cusp points of fold bifurcation curves, corresponding to fold codimension two singularities denoted C^j_k.
2. tangential points of a flip curve and a fold curve $(S_1 = -S_2 = +1)$ denoted NP_i, i is the number of the point.

Such points are related to the occurrence of the second condition both in eq. (2) and eq. (3), which thus lead to [4]:

$$N = d = 0. \tag{7}$$

The plan of the paper is as follows. In section 2, the fixed points are calculated and their stability is studied. We give transcritical, pitchfork and flip bifurcation curves of fixed points and period two cycles, which are obtained analytically or numerically. In section 3, we give the bifurcation structures in the parameter plane (a, b), as their evolution by variation of the third parameter c. The section 4 is devoted to synchronization and antisynchronization phenomena.

2. Definition of the Coupled Map

Let us consider the map T, defined as follows:

$$T : \begin{cases} x_{n+1} = F(x_n, y_n) = f_a(x_n) + (1 - c)bg(x_n,\ y_n), \\ y_{n+1} = G(x_n, y_n) = f_a(y_n) + bg(y_n,\ x_n), \end{cases} \tag{8}$$

Where $(x, y) \in [0, 1] \times [0, 1]$.
Uncoupled one-dimensional ($1D$) maps f_a given:

$$f_a(x) = x + \frac{a}{2\pi}\sin(2\pi x), \tag{9}$$

g is a coupling function of the form:

$$g(x, y) = \frac{1}{2\pi}\sin(2\pi(y - x)). \tag{10}$$

a is the control parameter of the uncoupled $1D$ map f_a.
b is a coupling parameter between the two subsystems and c $(0 \leq c \leq 1)$ is a parameter tuning the degree of asymmetry. The case of $c = 0$ [10, 12, 20, 21] corresponds to a symmetrical coupling; $c = 1$ corresponds to an unidirectional non symmetrical coupling [22, 23, 26].

3. Fixed Points

The fixed points of T verify $T(X) = X$. First, T has an infinite number of fixed points whose coordinates are given by the following equation:

$$P^* = (x^*, y^*) = \frac{1}{2}(k,\ l),\ \ k,\ l \in \mathbb{Z} \tag{11}$$

Note that all these fixed points (x^*, y^*) are independent of the parameters a, b, and c. Their coordinates are different regarding the parity of k and l.

There are four different types of such points depending on the parity of the integers (k, l), which appear in Eq. (11).

$$\begin{cases} P_1^* = (x^*, y^*) = (k, l), (k, l) \in \mathbb{Z}^2, \\ P_2^* = (x^*, y^*) = \frac{1}{2}(k, l), k = 2k^{'} + 1, l = 2l^{'} + 1, \\ (k^{'}, l^{'}) \in \mathbb{Z}^2, \\ P_3^* = (x^*, y^*) = (\frac{1}{2}k, l), k = 2k^{'} + 1, (k^{'}, l) \in \mathbb{Z}^2, \\ P_4^* = (x^*, y^*) = (k, \frac{1}{2}l), l = 2l^{'} + 1, (k, l^{'}) \in \mathbb{Z}^2. \end{cases} \tag{12}$$

We'll study them in a deeper way in the next paragraph, which concerns the stability of fixed points.

Moreover, there are eight fixed points dependent of a, b, and c, which are $P_1 = (x_1^*, y_1^*)$, $P_2 = (y_1^*, x_1^*)$, $P_3 = (x_2^*, y_2^*)$, $P_4 = (y_2^*, x_2^*)$, $P_5 = (x_2^*, y_1^*)$, $P_6 = (y_1^*, x_2^*)$, $P_7 = (y_2^*, x_1^*)$, $P_8 = (x_1^*, y_2^*)$.

Let us define:

$$A = \sqrt{b^2(2a^2 - b^2c^2)(c - 2)^2 + a^2(4b^2c - a^2)} \tag{13}$$

Then:

$$\begin{cases} x_1^* = \frac{1}{2\pi}\arctan(\frac{A}{2(c-1)ab}, \frac{-a^2 - b^2c(c-2)}{2(c-1)ab}) \\ y_1^* = \frac{1}{2\pi}\arctan(\frac{-A}{2(c-1)ab}, \frac{-a^2 - b^2c(c-2)}{2(c-1)ab}) \end{cases} \tag{14}$$

$$\begin{cases} x_2^* = \frac{1}{2\pi}\arctan(\frac{-A}{ab}, \frac{a^2 - b^2c(c+2)}{ab}) \\ y_2^* = \frac{1}{2\pi}\arctan(\frac{A}{ab}, \frac{a^2 - b^2c(c+2)}{ab}) \end{cases} \tag{15}$$

with:

$$\arctan(u, v) = -i\ln\frac{u + iv}{\sqrt{u^2 + v^2}} \tag{16}$$

The fixed points P_i,$i = 1, ..., 8$ exist, that means that they have real coordinates values, if (a, b) belongs to the hatched regions in Figure 1.

For other (a, b) values, fixed points P_i, $i = 1, ..., 8$ have complex coordinates or are rejected towards infinity.

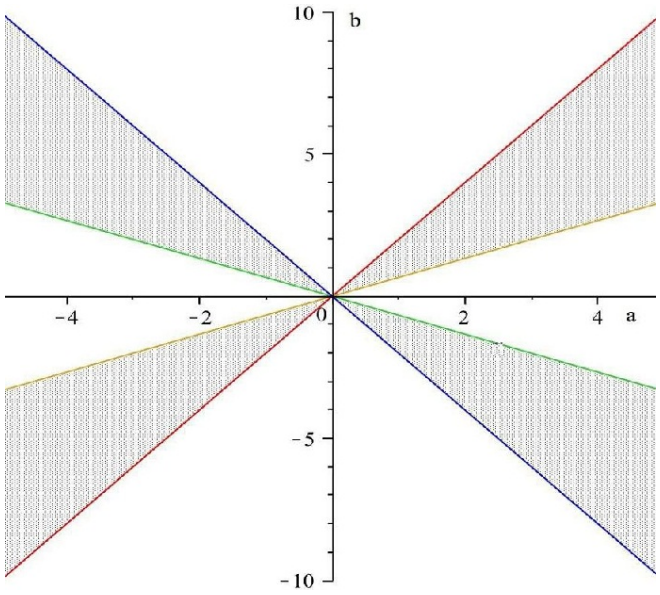

Figure 1. *Hatched regions in the parameter plane (a, b) correspond to the existence of real fixed points P_i, $i = 1, ..., 8$ for $c = \frac{1}{2}$.*

3.1. Stability of Fixed Points

To study the stability of fixed points, we need to calculate the eigenvalues of the Jacobian matrix at these points. The Jacobian matrix DT of T is a function of the states (x, y):

$$DT(x, y) = \begin{bmatrix} C & (1 - c)b\cos(2\pi(y - x)) \\ b\cos(2\pi(x - y)) & B \end{bmatrix} \tag{17}$$

with

$$C = 1 + a\cos(2\pi x) - (1 - c)b\cos(2\pi(y - x)) \tag{18}$$

$$B = 1 + a\cos(2\pi y) - b\cos(2\pi(x - y)) \tag{19}$$

First, we study the stability of the fixed points given by (13) to know their bifurcations.

1. At the fixed points $P_1^* = (x^*, y^*) = (k, l)$, $k, l \in \mathbb{Z}$, the eigenvalues of $DT(P_1^*)$ are:

$$S_1 = 1 + a \text{ and } S_2 = 1 + a - 2b + bc \tag{20}$$

2. At the fixed points $P_2^* = (x^*, y^*) = \frac{1}{2}(k, l)$, $k = 2k^{'} + 1, l = 2l^{'} + 1, (k^{'}, l^{'}) \in \mathbb{Z}^2$, i.e. k, l are odd, the eigenvalues of $DT(P_2^*)$ are:

$$S_1 = 1 - a \text{ and } S_2 = 1 - a - 2b + bc \tag{21}$$

3. At the fixed points $P_3^* = (x^*, y^*) = (\frac{1}{2}k, l)$, $k = 2k^{'} + 1, (k^{'}, l) \in \mathbb{Z}^2$, i.e. k is odd, the eigenvalues of $DT(P_3^*)$ are:

$$S_{1,\,2} = 1 + b - \frac{1}{2}bc \pm \frac{1}{2}\sqrt{(bc - 2c)^2 + 4a(a + bc)} \tag{22}$$

4. At the fixed points $P_4^* = (x^*, y^*) = (k, \frac{1}{2}l)$, $l = 2l^{'} + 1, (k, l^{'}) \in \mathbb{Z}^2$, i.e. l is odd, the eigenvalues of $DT(P_4^*)$ are:

$$S_{1,\,2} = 1 + b - \frac{1}{2}bc \pm \frac{1}{2}\sqrt{(bc - 2c)^2 - 4a(a + bc)} \tag{23}$$

Then, we study the stability of fixed points P_i, $i = 1, ..., 8$ given by Eq. (14) and Eq. (15), whose coordinates depend on the parameters.

5. At the fixed points P_i, $i = 1, ..., 8$, the eigenvalues of $DT(P_i)$ are:

$$S_{1,\,2} = \frac{1}{2(c-1)b}(-b^2c^2 + 3b^2c - 2b^2 - 2b + 2bc \pm \sqrt{E}) \tag{24}$$

with:

$$E = (6c^4 - 14c^3 + 4 - 12c + 17c^2 - c^5)b^4 + (-6c^2a^2 + 8ca^2 - 4a^2 + 2c^3a^2)b^2 + a^4(1 - c) \tag{25}$$

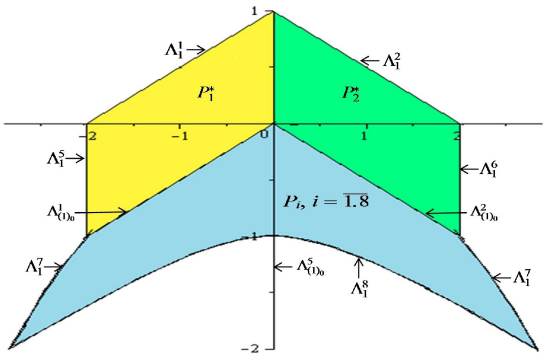

Figure 2. *Existence domaines of attracting fixed points in the parameter plane* (a, b) *for* $c = 0$.

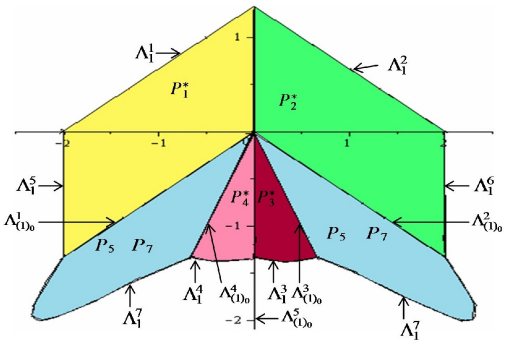

Figure 3. *Existence domaines of attracting fixed points in the parameter plane* (a, b) *for* $c = \frac{1}{2}$.

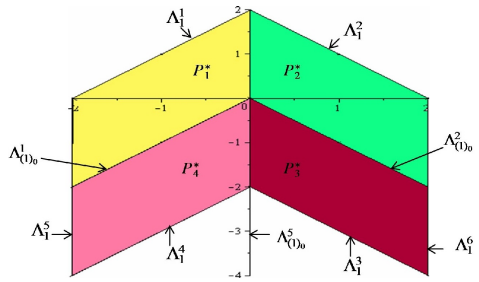

Figure 4. *Existence domaines of attracting fixed points in the parameter plane* (a, b) *for* $c = 1$.

3.2. Regions of the Stability

Figures 2, 3 and 4 represent the stability areas of these fixed points for $c = 0$, $c = \frac{1}{2}$ and $c = 1$ respectively.

1. For $c = 0$ the fixed points P_1^* are stable for $a \in]-2, 0[$ and $b \in]\frac{1}{2}a, 1 + \frac{1}{2}a[$, P_2^* are stable for $a \in]0, 2[$, $b \in]-\frac{1}{2}a, 1 - \frac{1}{2}a[$, P_3^*, P_4^* are unstable whatever be (a, b), and P_i are stable for $a \in]-2.828, 0[$, $b \in]-\frac{1}{2} - \frac{1}{2}\sqrt{1 + a^2}, \frac{1}{2}a[$ and $a \in]0, 2.828[$, $b \in]-\frac{1}{2} - \frac{1}{2}\sqrt{1 + a^2}, -\frac{1}{2}a[$ (see Figure 2).
2. For $c = \frac{1}{2}$ the fixed points P_1^* are stable for $a \in]-2, 0[$, $b \in]0, \frac{4}{3} + \frac{2}{3}a[$ and $a \in]-2, 0[$, $b \in]\frac{2}{3}a, 0[$, P_2^* are stable for $a \in]0, 2[$, $b \in]\frac{4}{3} - \frac{2}{3}a, 0[$, and $a \in]0, 2[$, $b \in]\frac{-2}{3}a, 0[$, P_3^* are stable for $a \in]0, \frac{2}{3}[$, $b \in]-2a, \frac{2(a^2-4)}{6-a}[$ and P_4^* are stable for $a \in]-\frac{2}{3}, 0[$, $b \in]\frac{2(a^2-4)}{6+a}, 0[$ (see Figure 3).

3. For $c = 1$ the fixed points P_1^* are stable for $a \in]-2, 0[$, $b \in]a, 2+a[$, P_2^* are stable for $a \in]0, 2[$, $b \in]-a, 2-a[$, P_3^* are stable for $a \in]0, 2[$, $b \in]-(2+a), a[$ and P_4^* are stable for $a \in]-2, 0[$, $b \in]-(2-a), a[$ (see Figure 4).

4. Bifurcation Structure

In this section, we present the study of bifurcations in the parameter plane (a, b), (the parameter c is fixed). A bifurcation is a qualitative change of the system behavior when a parameter varies [8, 24, 25, 27]. This change may correspond to the appearance or disppearance of new singularities, or a change in the nature of singularities [6]. We can define different kinds of bifurcations for fixed points and period two cycles as, saddle-node, period doubling, transcritical or pitchfork bifurcations [9, 12, 24]. The study of the sequence of bifurcations permits to understand the mechanisms that lead to chaos.

Figures 5, 6 and 7 represent the stability domaines obtained by numerical simulations for the transformation T in the parameter plane (a, b) for $c = 0$, $c = \frac{1}{2}$ and $c = 1$, respectively. Each colored region corresponds to the existence of a stable periodic orbit with period indicated in the bar on the bottom of the figure. When b is changed, we can remark that some stability regions are periodically repeated (Figure 7).

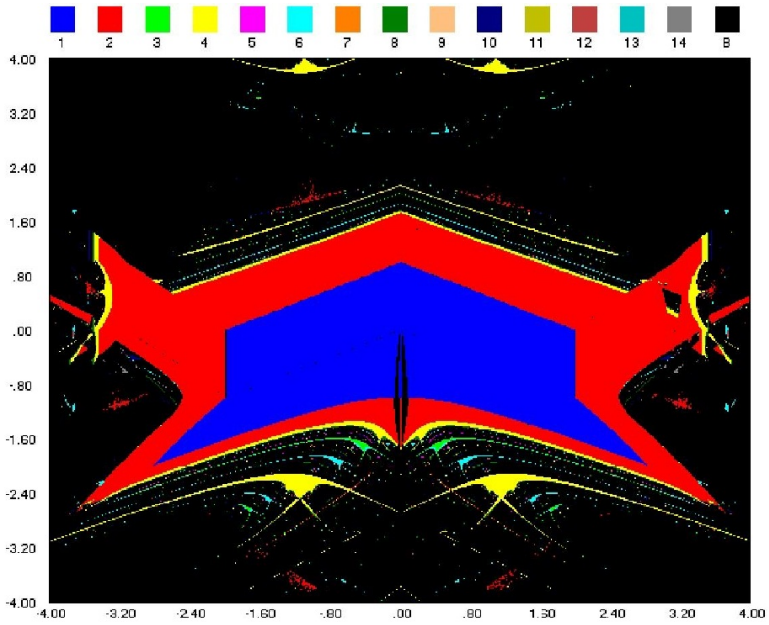

Figure 5. *Existence domaines of attracting cycles in the parameter plane (a, b), for the map T when $c = 0$. Each colored part corresponds to the existence of a stable cycle (periodic point), the period k (period) of which is given by the upper colored squares. The black color corresponds to the cycles period $k \geq 15$ or to chaos.*

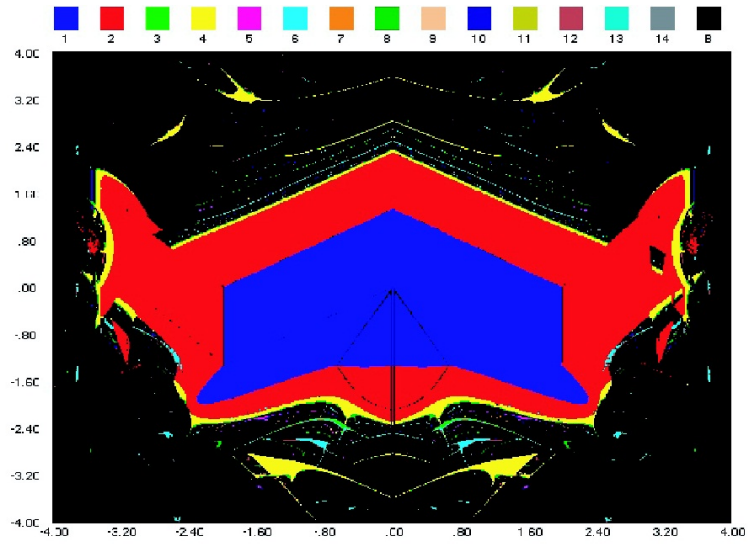

Figure 6. *Existence domaines of attracting cycles in the parameter plane (a, b) for the map T when $c = \frac{1}{2}$.*

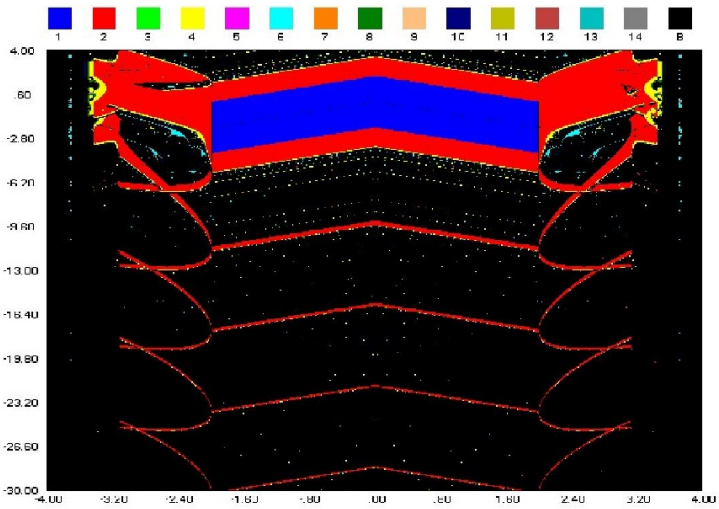

Figure 7. *Existence domaines of attracting cycles in the parameter plane* (a, b) *for the map* T *when* $c = 1$.

4.1. Singular Points of Codimension Two

From Eq. (7), we obtain six singular points whose coordinates are:

$$\begin{cases} NP_1 : a = -2,\ b = \frac{2}{c-2}, \\ NP_2 : a = 2,\ b = \frac{2}{c-2}, \\ NP_3 : a = \frac{-2c}{c-2},\ b = \frac{2}{c-2}, \\ NP_4 : a = \frac{2c}{c-2},\ b = \frac{2}{c-2}, \\ NP_5 : a = 0,\ b = \frac{-2}{c-2}, \\ NP_6 : a = 0,\ b = \frac{2}{c-2} \end{cases} \tag{26}$$

4.2. Bifurcation Curves

We can also obtain analytically some bifurcation curves for fixed points and period 2 cycles. The equation of a transcritical or pitchfork bifurcation curve $\Lambda^j_{(1)_0}$ for a fixed point of coordinates (x, y) is:

$$\begin{aligned} &\Lambda^j_{(1)_0} : -b\cos(2\pi(x-y)) + a^2\cos(2\pi x)\cos(2\pi y) - a\cos(2\pi x)b\cos(2\pi(x-y)) - b\cos(2\pi(x-y))a\cos(2\pi y) \\ &+bc\cos(2\pi(y-x)) + bca\cos(2\pi(y-x))\cos(2\pi y) + \\ &(1-c)b\cos(2\pi(y-x)) = 0. \end{aligned} \tag{27}$$

The equation of a flip bifurcation curve $\Lambda^{j'}_1$ for a fixed point of coordinates (x, y) is:

$$\begin{aligned} &\Lambda^{j'}_1 : -4 - 2a\cos(2\pi y) + 3b\cos(2\pi(x+-y)) - 2a\cos(2\pi x) \\ &-a^2\cos(2\pi x)\cos(2\pi y) + ab\cos(2\pi x)\cos(2\pi(x-y)) \\ &+ab\cos(2\pi(x-y))\cos(2\pi y) - bc\cos(2\pi(x-y)) \\ &-bca\cos(2\pi(x-y))\cos(2\pi y) + (1-c)b\cos(2\pi(y-x)) = 0. \end{aligned} \tag{28}$$

Then the equations of transcritical and pitchfork bifurcation curves $\Lambda^j_{(1)_0}, j = 1, ..., 5$ for the fixed points $P^*_i, i = 1, ..., 4$ are respectively:

$$\begin{aligned} \text{Pitchfork} : &\begin{cases} P^*_1 : \Lambda^1_{(1)_0} : b = \frac{a}{2-c} \\ P^*_2 : \Lambda^2_{(1)_0} : b = \frac{a}{c-2} \\ P^*_3 : \Lambda^3_{(1)_0} : b = -\frac{a}{c} \\ P^*_4 : \Lambda^4_{(1)_0} : b = \frac{a}{c} \end{cases} \\ \text{Transcritical} : &\left\{ P^*_i, i = 1, ..., 4 : \Lambda^5_{(1)_0} : a = 0 \right. \end{aligned} \tag{29}$$

The $\Lambda^{j}_{(1)_0}$, $j = 1, ..., 4$ are a pitchfork bifurcation curves for the fixed points P^*_i, $i = 1, ..., 4$ respectively.

Transcritical bifurcation curve $\Lambda^{5}_{(1)_0}$ is related to the four points P^*_i, $i = 1, ..., 4$.

The equations of flip bifurcations curves Λ^{j}_1, $j = 1, ..., 6$ for fixed points P^*_i, $i = 1, ..., 4$ are respectively:

$$\text{Flip bifurcations}: \begin{cases} P^*_1: \begin{cases} \Lambda^1_1 : b = \frac{a+2}{2-c} \\ \Lambda^5_1 : a = -2, \end{cases} \\ P^*_2: \begin{cases} \Lambda^2_1 : b = \frac{a-2}{c-2} \\ \Lambda^6_1 : a = 2, \end{cases} \\ P^*_3 : \Lambda^3_1 : b = \frac{a^2-4}{-4+2c+ca}, \\ P^*_4 : \Lambda^4_1 : b = \frac{a^2-4}{4-2c+ca} \end{cases} \tag{30}$$

The presence of a transcritical bifurcation has important consequences for the dynamics of the system (4), it is a special case of a bifurcation ($S_i = +1$, $i = 1$ or 2). At the bifurcation point the fixed points exchange their stability. Beyond the bifurcation point the number of fixed points has not changed contrary to a fold bifurcation where two fixed points appear or disappear. Pitchfork bifurcations are also possible in the dynamics of the system (4), pitchfork bifurcations are the generic bifurcations when such a symmetric fixed point changes its stability. Two fixed points with a broken symmetry bifurcate at once in a pitchfork bifurcation. Both are either stable (supercritical pitchfork bifurcation) or unstable (subcritical pitchfork bifurcation).

In this paper, we present the transcritical and pitchfork bifurcations (stable and unstable) in the parameter plane (a, b) for $0 \leq c \leq 1$.

We have plotted the flip, transcritical and pitchfork bifurcation curves of fixed points, the singularity points NP_i, $i = 1, ..., 6$ and the flip and fold bifurcation curves of the period 2 cycles in the parameter plane (a, b) for the following three cases, $c = 0$ (symmetrical coupling), $0 < c < 1$ (non-symmetrical coupling), $c = 1$ (non-symmetrical and unidirectional coupling).

Case 1: $c = 0$

From Eq. (29) and Eq. (30), we analytically obtain the parametric equations of transcritical, pitchfork and flip bifurcation curves of fixed points, $\Lambda^{j}_{(1)_0}$, $j = 1, 2, 5$, and $\Lambda^{j'}_1$, $j' = 1, ..., 6.$.

Moreover, we can obtain three more bifurcation curves related to the fixed points P_i, $i = 1, ..., 8$:

$$\begin{cases} \Lambda^7_1 : b = -\frac{1}{4}a^2 \\ \Lambda^8_1 : b = -\frac{1}{2} - \frac{1}{2}\sqrt{1+a^2} \\ \Lambda^9_1 : b = -\frac{1}{2} + \frac{1}{2}\sqrt{1+a^2} \end{cases} \tag{31}$$

Those equations are only analytically obtained for $c = 0$, otherwise, they are too complex to be solved analytically. From Eq. (26), we obtain the coordinates of codimension two points. In Figure 8, we can see the bifurcation curves in the parameter plane (a,b) and the location of the singularity points NP_i, $i = 1, ..., 6$. Let us remark that $NP_3 \equiv NP_4$. $\Lambda^{1}_{(1)_0}$, $\Lambda^{2}_{(1)_0}$, and $\Lambda^{5}_{(1)_0}$ are straight lines passing through (0, 0), the curves $\Lambda^{3}_{(1)_0}$ and $\Lambda^{4}_{(1)_0}$ tends to infinity (see Eq. (29)). Flip bifurcation curves Λ^1_1, Λ^2_1, Λ^5_1, and Λ^6_1 corresponding to P^*_1 and P^*_2 are straight lines, Λ^3_1 corresponding to the fixed point P^*_3 and Λ^4_1 corresponding to the fixed point P^*_4 are merged and correspond to a parabola. Curves Λ^7_1, Λ^8_1, and Λ^9_1 for P_i, $i = 1, ..., 8$ are also parabolic.

Figures 9 and 10 represent the characteristic bifurcation curves of period 2 cycles respectively flip and fold. All these curves have been numerically obtained.

We note that there is a symmetry of the bifurcation curves for fixed points and period 2 cycles relatively to the b-axis. Some bifurcation curves correspond to boundaries of stability domaines given in Figure 5 in the (a,b) plane. Some bifurcation curves plotted in Figures 2 and 8 limit the stability domaines of fixed points (blue area in Figure 5) and some curves plotted in Figures 9 and 10 limit the stability domaines of period 2 cycles (red areas in Figure 5).

In Figure 11, we present the transcritical and pitchfork bifurcation curves of fixed points P^*_1, P^*_2 and P_i, $i = 1, ..., 8$. Both before and after the bifurcation, there is one unstable and one stable fixed point. However, their stability is exchanged when they collide. So the unstable fixed point becomes stable and vice versa. Similarly, the Figure 11 shows the existence of the following bifurcations:

1. Transcritical bifurcation between $P^*_1 \leftrightarrow P^*_2$ to passage $\Lambda^{5}_{(1)_0}$
2. Pitchfork bifurcation (stable and unstable) around P^*_1 to passage $\Lambda^{1}_{(1)_0}$.

$$P^*_1 \; N_S(\text{resp.}N_I) \leftrightarrow 2N_S(\text{resp.}2N_I) + C \; (\text{resp.}C) \tag{32}$$

3. Pitchfork bifurcation (stable and unstable) around P^*_2 to passage $\Lambda^{2}_{(1)_0}$.

$$P^*_2 \; N_S(\text{resp.}N_I) \leftrightarrow 2N_S(\text{resp.}2N_I) + C \; (\text{resp.}C) \tag{33}$$

P^*_i (N_S) denotes a fixed point P^*_i of type stable node, and P^*_i (N_I) denotes a fixed point P^*_i of type unstable node.

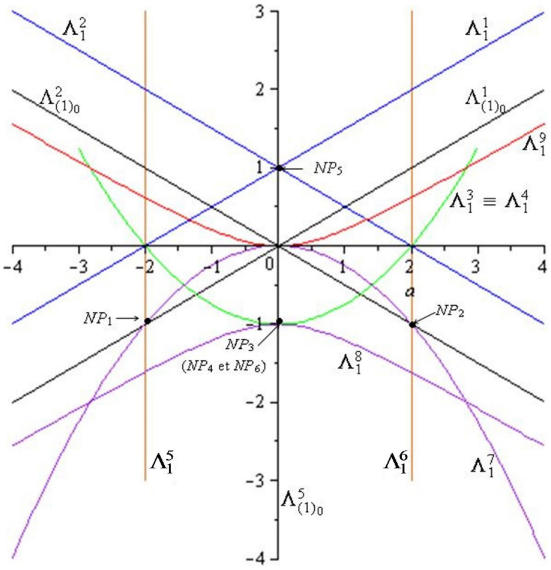

Figure 8. *Flip, transcritical and pitchfork bifurcation curves of fixed points for T, when* $c = 0$.

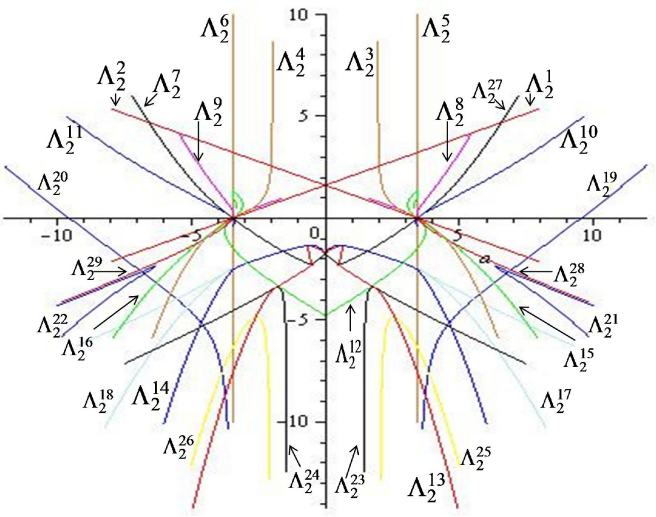

Figure 9. *Flip bifurcation curves of period* 2 *cycles, when* $c = 0$.

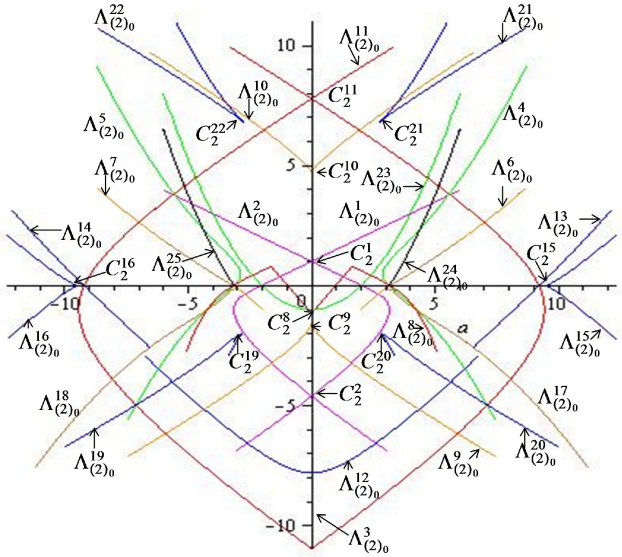

Figure 10. *Fold bifurcation curves of period* 2 *cycles, when* $c = 0$.

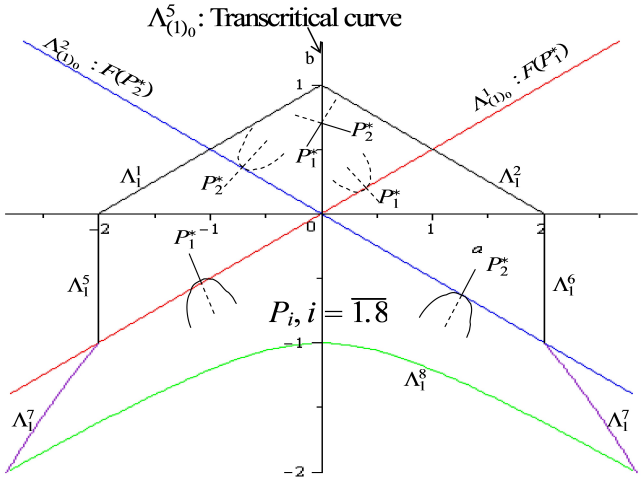

Figure 11. *Transcritical and pitchfork bifurcation curves of fixed points for* T *in the parameter plane* (a, b), *when* $c = 0$, *obtained from eq.* (29).

Case 2: $0 < c < 1$

Without loss of generality, we have chosen to study the curves when $c = \frac{1}{2}$. We also obtain analytically and numerically the flip, transcritical and pitchfork bifurcation curves. For fixed points, the equations of fold bifurcation curves $\Lambda^j_{(1)_0}$, $j = 1, ..., 5$ are given from Eq. (29) and the equations of flip bifurcation curves $\Lambda^{j\prime}_1$,$j\prime = 1, ..., 6$ from (30). The coordinates of points of codimension two are analytically obtained from Eq. (26).

In the parametric plane (a, b), we represent the transcritical, pitchfork and flip bifurcation curves of fixed points (see Figure 12). $\Lambda^j_{(1)_0}$, $j = 1, ..., 5$, are straight lines passing through (0, 0). Λ^1_1, Λ^2_1, Λ^5_1, Λ^6_1 are also straight lines. Λ^3_1, Λ^4_1, Λ^9_1 are parabolic curves. Λ^7_1 is a closed curve and Λ^8_1 tends to $-\infty$. In the same figure, we give the locations of points of codimension two NP_i, $i = 1, ..., 6$.

Figures 13 and 14 represent the bifurcation curves of period 2 cycles respectively flip and fold. Figure 15 represents the transcritical and pitchfork bifurcation curves corresponding to this case, we can remark in Figure 15 the following bifurcations:

1. Transcritical bifurcation between $P^*_1 \leftrightarrow P^*_2$ to passage $\Lambda^5_{(1)_0}$.
2. Transcritical bifurcation between $P^*_3 \leftrightarrow P^*_4$ to passage $\Lambda^5_{(1)_0}$.
3. Pitchfork bifurcation (stable and unstable) around P^*_1 to passage $\Lambda^1_{(1)_0}$.

$$P^*_1\ N_S\ (\text{resp. } N_I) \leftrightarrow 2N_S\ (\text{resp. } 2N_I) + C\ (\text{resp. } C) \quad (34)$$

4. Pitchfork bifurcation (stable and unstable) around P^*_2 to passage $\Lambda^2_{(1)_0}$.

$$P^*_2\ N_S\ (\text{resp. } N_I) \leftrightarrow 2N_S\ (\text{resp. } 2N_I) + C\ (\text{resp. } C) \quad (35)$$

5. Pitchfork bifurcation (stable and unstable) around P^*_3 to passage $\Lambda^3_{(1)_0}$.

$$P^*_3\ N_S\ (\text{resp. } N_I) \leftrightarrow 2N_S\ (\text{resp. } 2N_I) + C\ (\text{resp. } C) \quad (36)$$

6. Pitchfork bifurcation (stable and unstable) around P^*_4 to passage $\Lambda^4_{(1)_0}$.

$$P^*_4\ N_S\ (\text{resp. } N_I) \leftrightarrow 2N_S\ (\text{resp. } 2N_I) +\ C\ (\text{resp. } C) \quad (37)$$

As in the case $c = 0$, some bifurcation curves correspond to boundaries of stability domaines given in Figure 6 in the (a,b) plane. Some bifurcation curves plotted in Figures 3 and 12 limit the stability domaines of fixed points (blue area in Figure 6) and some curves plotted in Figures 13 and 14 limit the stability domaines of period 2 cycles (red areas in Figure 6).

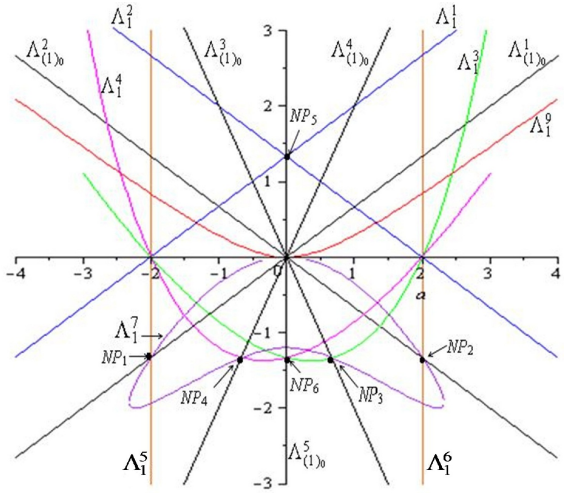

Figure 12. *Flip, transcritical and pitchfork bifurcation curves of fixed points for T, when $c = \frac{1}{2}$.*

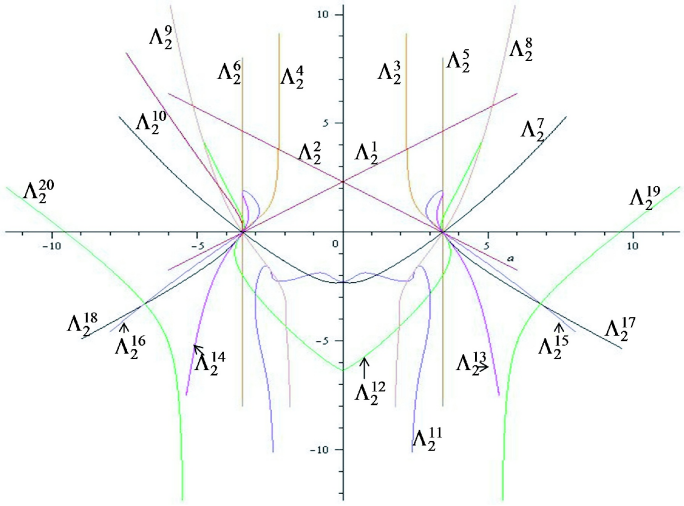

Figure 13. *Flip bifurcation curves of period 2 cycles, when $c = \frac{1}{2}$.*

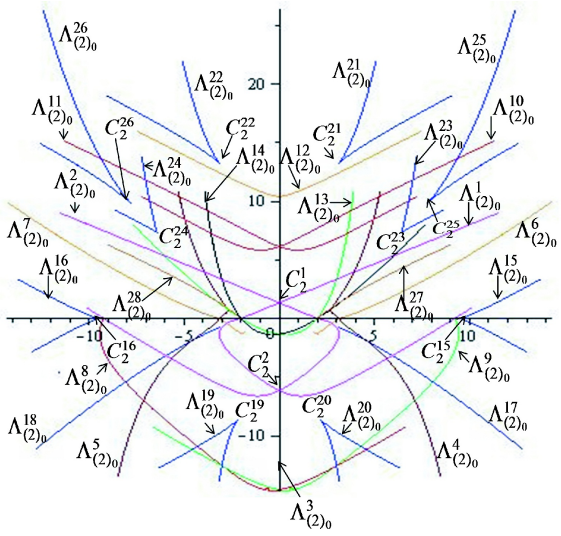

Figure 14. *Fold bifurcation curves of period 2 cycles, when $c = \frac{1}{2}$.*

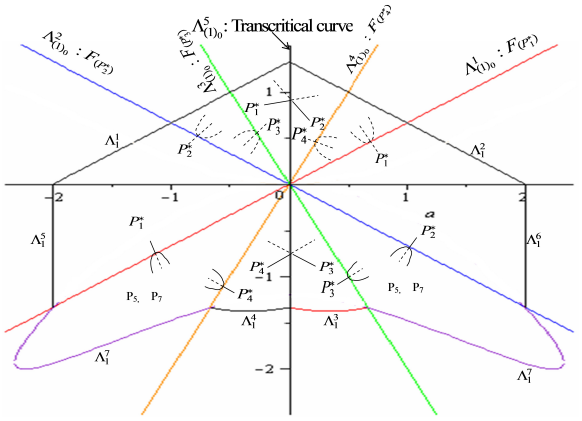

Figure 15. *Transcritical and pitchfork bifurcation curves of fixed points for T in the parameter plane (a, b), when $c = \frac{1}{2}$.*

Case 3: $c = 1$

In the case of the non-symmetric and unidirectional coupling of T, we can also analyze the local bifurcations, flip, transcritical and pitchfork of fixed points. We obtain analytically the transcritical, pitchfork and flip bifurcation curves regarding fixed points from equations Eq. (29) and Eq. (30). We have plotted these curves in the parametric plane (a, b) in Figure 17. The bifurcation curves $\Lambda^1_{(1)_0}$, $\Lambda^2_{(1)_0}$ and Λ^1_i, $i = 1, ..., 6$ are straight lines. The curve $\Lambda^4_{(1)_0}$ merges into $\Lambda^1_{(1)_0}$, and $\Lambda^3_{(1)_0}$ merges into $\Lambda^2_{(1)_0}$. We notice the absence of bifurcation curves Λ^7_1, Λ^8_1, and Λ^9_1, because the fixed points P_i, $i = 3, 4, 8$, have complex coordinates, and the points P_i, $i = 1, 2, 5, 6, 7$ tend to infinity. The coordinates of codimension-two points are obtained from Eq. (26) and we present the location of these points also in Figure 17. Let us remark that $NP_1 \equiv NP_4$ and $NP_2 \equiv NP_3$.

Using numerical methods, we have plotted the bifurcation curves for period 2 cycles in the parameter plane (a, b); Figures 18 and 19 show, respectively, flip and fold bifurcation curves. Some bifurcation curves correspond to the boundaries of stability domaines in the plane (a, b) given in Figure 7. Some bifurcation curves plotted in Figures 4 and 17 limit the stability domaines of fixed points (blue area in Figure 7) and some curves plotted in Figures 18 and 19 limit the stability domaines of period 2 cycles (red areas in Figure 7). We can also see that the bifurcation curves of period 2 cycles are repeating periodically. We note that there is a symmetry of the bifurcation curves for fixed points and period 2 cycles relatively to the coupling parameter b, although the transformation in this case is non symmetric and the coupling is unidirectional. Figure 20 shows the transcritical and pitchfork bifurcation curves of fixed points P^*_i , $i = 1, ..., 4$. Where $c = 1$, only the fixed points P^*_i , $i = 1, ..., 4$ exist. And we also have in Figure 20 the following bifurcations:

1. Transcritical bifurcation between $P^*_1 \leftrightarrow P^*_2$ to passage $\Lambda^5_{(1)_0}$.
2. Transcritical bifurcation between $P^*_3 \leftrightarrow P^*_4$ to passage $\Lambda^5_{(1)_0}$.
3. Pitchfork bifurcation (stable and unstable) around P^*_1 and P^*_4 to passage $\Lambda^1_{(1)_0}$.

$$\begin{cases} P_1^* \; N_S \text{ (resp. } N_I) \leftrightarrow 2N_S \text{ (resp. } 2N_I) + \; C \text{ (resp. } C) \\ P_4^* \; N_S \text{ (resp. } N_I) \leftrightarrow 2N_S \text{ (resp. } 2N_I) + \; C \text{ (resp. } C) \end{cases} \tag{38}$$

1. Pitchfork bifurcation (stable and unstable) around P_2^* and P_3^* to passage $\Lambda^2_{(1)_0}$.

$$\begin{cases} P_2^* \; N_S \text{ (resp. } N_I) \leftrightarrow 2N_S \text{ (resp. } 2N_I) + \; C \text{ (resp. } C) \\ P_3^* \; N_S \text{ (resp. } N_I) \leftrightarrow 2N_S \text{ (resp. } 2N_I) + \; C \text{ (resp. } C) \end{cases} \tag{39}$$

4.3. Evolution of the Flip Bifurcation Curves for P_i When the Third Parameter c Varies

Now, let us have a look on the evolution of the flip bifurcation curves Λ_1^7, Λ_1^8, and Λ_1^9 corresponding to the fixed points P_i, $i = 1, ..., 8$, for increasing values of the third parameter c from $c = 0$ to $c = 1$, with $(a, b) \in [-5, 5]^2$ (see Figures 16).

The bifurcation value $c = 0.0355730$ (Figure 16(a)) corresponds to a new contact between Λ_1^7 and Λ_1^8 at points α_1 and α_2. After this bifurcation, when $c = 0.0355731$ the Λ_1^7, Λ_1^8 are divided into three curves, a closed curve Λ_1^7, and Λ_1^8, $\Lambda_1^{8'}$ (Figures 16(b)-(c)). For $c = 0.99$, we can see another curve Λ_1^{10} (Figure 16(d)), which merges into Λ_1^9 for $c = 0.99999$; these two curves tends to the diagonal $b = a$ and the antidiagonal $b = -a$ (Figure 16(e)) before disappearing for $c = 1$ when merging into the point $(0, 0)$.

We can also see that, numerically, when c approaches 1, the curves Λ_1^8, $\Lambda_1^{8'}$ tends to $-\infty$.

We have plotted numerically bifurcation curves for fixed points and period 2 cycles. Even for these low period, the bifurcation structure is very rich and complex. So it will probably be the same for higher period of cycles. We can remark the good correspondence between the simulations of Figures 5, 6 and 7 and the bifurcation curves obtained for fixed points and period 2 cycles. All this study permits to have a better understanding of the evolution of attractors in the case of fixed points and period 2 cycles.

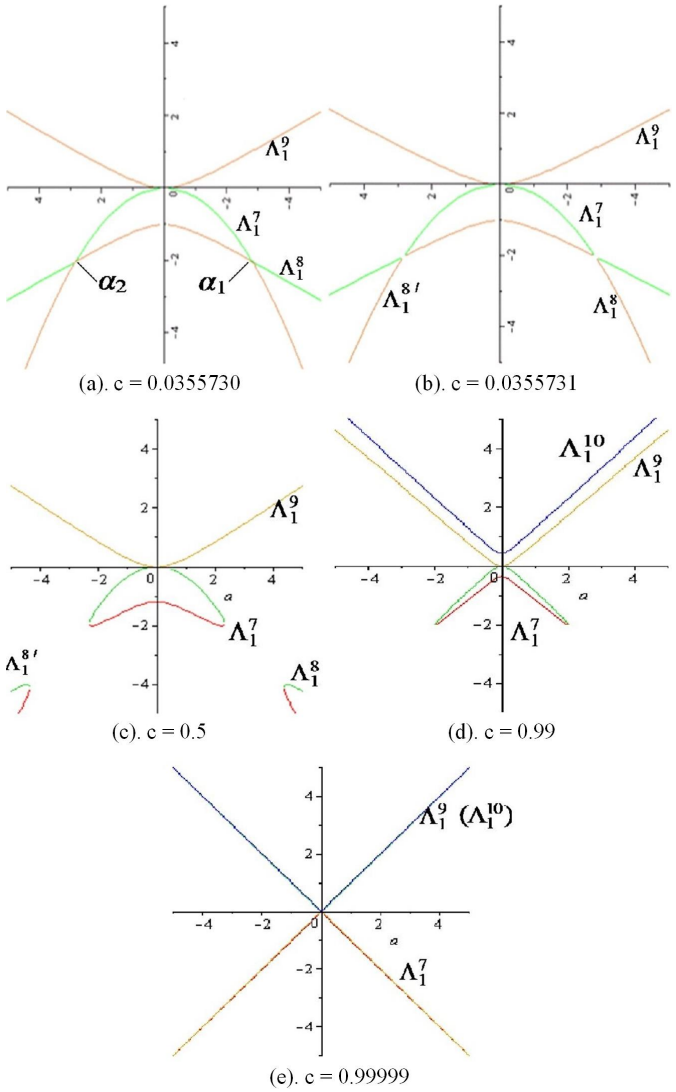

Figure 16. *Evolution of the bifurcation curves for fixed points P_i, $i = 1, ..., 8$ in the parametric plane (a, b) for different values of c.*

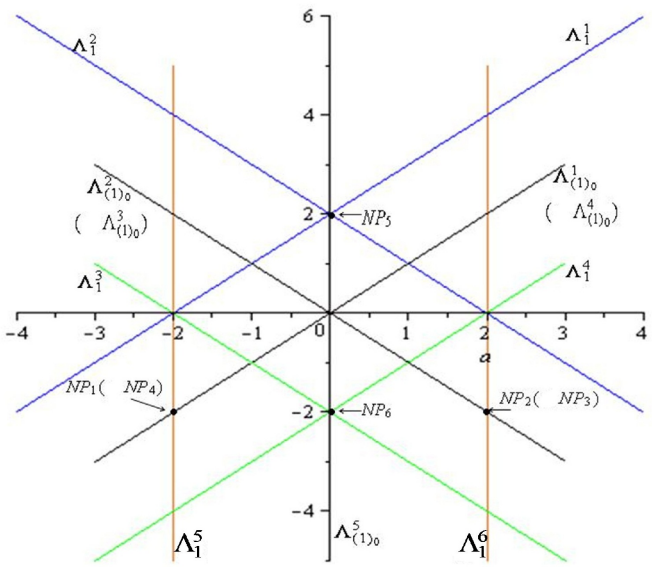

Figure 17. *Flip, transcritical and pitchfork bifurcation curves of fixed points for T, when $c = 1$.*

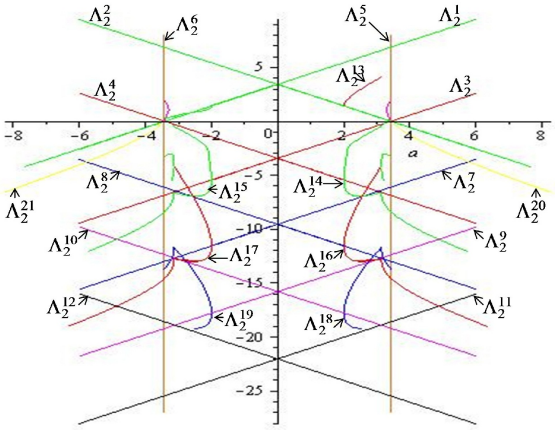

Figure 18. *Flip bifurcation curves of period 2 cycles, when $c = 1$.*

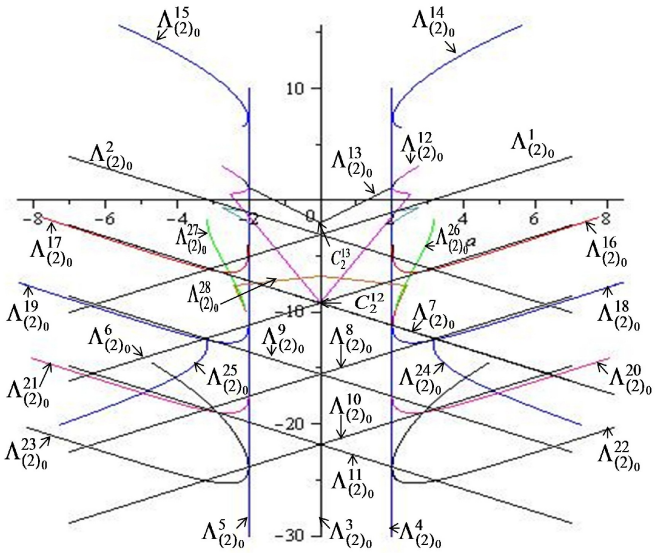

Figure 19. *Fold bifurcation curves of period 2 cycles, when $c = 1$.*

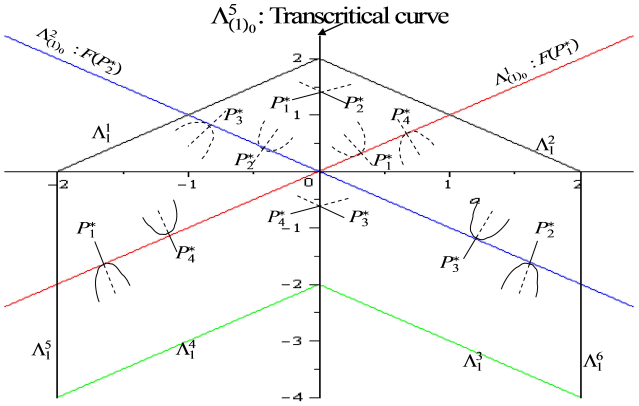

Figure 20. *Transcritical and pitchfork bifurcation curves of fixed points for T in the parameter plane (a, b), when $c = 1$.*

5. Synchronization and Antisynchronization of Coupled Map

We focus on the dynamics of T restricted to the invariant diagonal. Let $(x,\ x) \in \Delta$ and $(x_1,\ x_1) = T(x,\ x)$, then the restriction T/Δ to the diagonal is reduced to the one-dimensional map $f_a(x)$ (as in [12]), when $c = 0$):

$$x_1 = f_a(x) = x + \frac{a}{2\pi}\sin(2\pi x) \tag{40}$$

For $c = 0$, leading to $y_1 = 1 - x_1$. Let $(x,\ 1-x) \in \Delta_{-1}$ and $(x_1,\ y_1) = T(x,\ 1-x)$ then the restriction T/Δ_{-1} is:

$$T/\Delta_{-1} : \begin{cases} x_1 = f_a(x) - (1-c)\frac{b}{2\pi}\sin(4\pi x) \\ \\ y_1 = 1 - f_a(x) + \frac{b}{2\pi}\sin(4\pi x) \end{cases} \tag{41}$$

In Figures 21 and 22, we remark the existence of two synchronized four-band chaotic attractors, which are indicated by segments along the main diagonal Δ and correspond to synchronization phenomenon. Their basins of attraction (in cyan and magenta) are standard open sets [1, 2, 13].

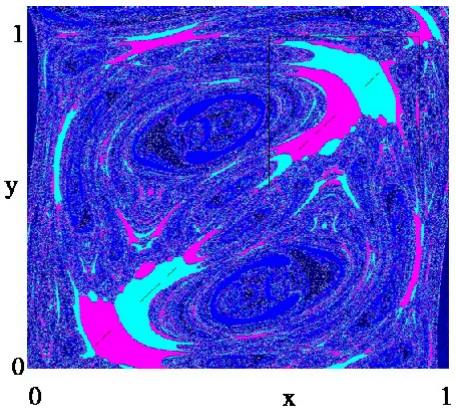

Figure 21. *Two synchronized four-band chaotic attractors coexist for $a = 3.54$, $b = 1.6$ and $c = 0.5$. Their basins are coloured in cyan and magenta.*

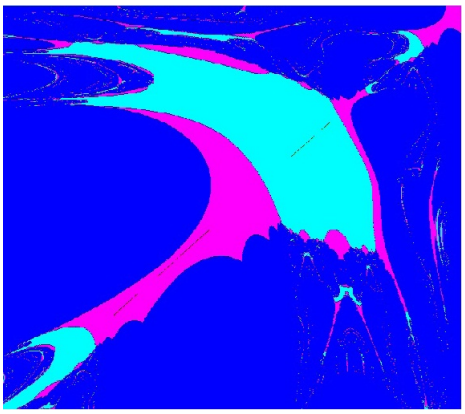

Figure 22. *Enlargment of Figure 21.*

6. Summary of Main Results

By varying the third parameter c of the map T, we have got to know the qualitative behavior of the system (4), and we can focus on the main results that we have obtained:

1. The transcritical bifurcation curve $\Lambda^5_{(1)_0} : a = 0$, always exists $\forall c \in [0, 1], \forall x, y \in \mathbb{R}$.
2. The flip bifurcation curves $\Lambda^5_1 : a = -2$ corresponding to the fixed point P^*_1 and $\Lambda^6_1 : a = 2$ corresponding to the fixed point P^*_2, always exist $\forall c \in [0, 1]$.
3. When $c = 0$, the fixed points P^*_3, P^*_4 are unstable $\forall(a, b) \in \mathbb{R}^2$. $\Lambda^3_{(1)_0}$ and $\Lambda^4_{(1)_0}$ tend to infinity.
4. When $0 < c < 1$, we note the presence of all transcritical and pitchfork bifurcation curves $\Lambda^j_{(1)_0}, j = 1, ..., 5$.
5. When $c = 1$, the fixed points P_i, $i = 3, 4, 8$, have complex coordinates, and other $P_i, i = 1, 2, 5, 6, 7$ tends to infinity, which implies the absence of bifurcations curves Λ^7_1, Λ^8_1 and Λ^9_1. The curve $\Lambda^3_{(1)_0}$ merges into $\Lambda^2_{(1)_0}$, and $\Lambda^4_{(1)_0}$ merges into $\Lambda^1_{(1)_0}$.
6. There is a symmetry of the bifurcation curves for fixed points and order 2 cycles relatively to the b-axis, $\forall c \in [0, 1]$.
7. Synchronization phenomenon exists $\forall c \in [0, 1]$.
8. Chaotic antisynchronization only exists for $c = 0$.

7. Conclusion

The bifurcations of the two-dimensional coupled map in parameter plane (a, b) gives rise to a structure that is very complex, we have presented here the fold bifurcation curves $(S_1 = +1)$ and the flip bifurcation curves $(S_1 = -1)$ for fixed points and period two cycles. We have studied the situations of the parametric singularities when $S_1 = -S_2 = +1$. We have also investigated the synchronization and antisynchronization in two coupled map T with an invariant diagonal $x = y$ and antidiagonal $y = 1 - x$, respectively. The results have been obtained via a mixing between analytical and numerical methods. Results concerning synchronizationand antisynchronization are very similar to that obtained in [12]. The introduction of a third parameter c has permitted to better understand the evolution of bifurcation structures and to generalize synchronization phenomena.

References

[1] J. C. Alexander, J. A. Yorke, Z. You, and I. Kan, (1992), "Riddled basins," Int. J. Bifurc. Chaos 2, 795-813.

[2] J. C. Alexander, B. R. Hunt, I. Kan, and J. A.Yorke, (1996) "Intermingled basins of the triangle map," Ergod. Th. Dyn. Syst. 16, 651-662.

[3] J.P. Carcasses, (1993), "Determination of different configurations of fold and flip bifurcation curves of a one or two-dimensional map," Int. J. Bifurc. Chaos Vol. 3, No 4, 869-902.

[4] J.P. Carcasses, (1995) "Singularities of the parametric plane of an n-dimensional map. Determination of different configurations of fold and flip bifurcation curves," Int. J. Bifurc. Chaos Vol. 5, No 2, 419-447.

[5] K. M. Cuomo and A. V. Oppenheim, (1993) "Circuit implementation of synchronized chaos with applications to communications," Phys. Rev. Lett. 71, 65-68.

[6] S. Dinar, (1994) "Etude des bifurcations d'une equation non autonome de Duffing-Rayleigh et d'un modulateur MICDIF," PhD These, Universite Paul Sabatier de Toulouse, No 1673.

[7] H. Fujisaka and T. Yamada, (1983) "Stability theory of synchronized motion in coupled-oscillator systems," Progr. Theor. Phys. 69, 32-46.

[8] L. Gardini, R. Abraham, R. J. Record and D. Fournier-Prunaret, (1994) "A double logistic map," Int. J. Bifurc. Chaos, Vol. 4, No. 1, 145-176.

[9] I. Gumowski and C. Mira, (1980) "Dynamique chaotique, transformations ponctuelles, transition ordre desordre," Ed. Ce padues.

[10] N. E. Hamri, Y. Soula, (2010) "Basins and critical curves generated by a family of two-dimensional sine maps," Electronic Journal of Theoretical Physics, EJTP 7, No. 24, 139-150.

[11] L. Kocarev, K. S. Halle, K. Eckert, L. O. Chua, and U. Parlity, (1992) "Transmission of Digital signals by chaotic synchronization," Int. J. Bifurc. Chaos, Appl. Sci. Eng. 2, 973-977.

[12] V. L. Maistrenko, YU. L. Maistrenko and E. Mosekilde, (2005), "Chaotic synchronization and antisynchronization in coupled sine maps," Int. J. Bifurc. Chaos Vol. 15, No 7, 2161-2177.

[13] Yu. L. Maistrenko, V. L. Maistrenko, A. Popovich and E. Mosekilde, (1998), "Transverse instability and riddled basins in a system of two coupled logistic maps," Phys. Rev. E57, 2713–2724.

[14] J. Leonel Rocha, Abdel-Kaddous Taha and D. Fournier-Prunaret, (2016), "Big Bang Bifurcation Analysis and Allee Effect in Generic Growth Functions," International Journal of Bifurcation and Chaos, Vol. 26, No. 6 1650108, (20 pages), World Scientific Publishing Company, DOI: 10.1142/S021812741650108 X.

[15] J. Leonel Rocha, Abdel-Kaddous Taha and D. Fournier-Prunaret, (2016), "Dynamical Analysis and Big Bang Bifurcations of 1D and 2D Gompertz's Growth Functions," International Journal of Bifurcation and Chaos, Vol. 26 , No 11 1630030, (22 pages), World Scientific Publishing Company, DOI: 10.1142/S0218127416300305.

[16] J. Leonel Rocha and Abdel-Kaddous Taha, (2019), "Allee's Effect Bifurcation in Generalized Logistic Maps", International Journal of Bifurcation and ChaosVol. 29 , No. 03,1950039.

[17] J. Leonel Rocha and Abdel-Kaddous Taha, (2019), "Bifurcation structures in a 2D exponential diffeomorphismwith Allee effect," Nonlinear Dyn 95:3357-3374, https://doi.org/10.1007/s11071-019-04759-3.

[18] J. Leonel Rocha, Abdel-Kaddous Taha and D. Fournier-Prunaret, (2020), "Dynamics and bifurcations of a map of homographic Ricker type," Nonlinear Dyn 102: 1129-1149 https://doi.org/ 10.1007 /s 11071-020-05820-2.

[19] L. Gardini, A, Garijo and X. Jarque, (2021), "Topological Properties of the Immediate Basins of Attraction for the Secant Method," Mediterr. J. Math. 18: 221 https://doi.org/10.1007/s00009-021-01845-y1660-5446/21/050001-27 published online September 7, 2021 The Author(s) 2021.

[20] C. Mira, and C. Gracio, (2003), "On the embedding of a (p-1)-dimensional noninvertible map into a pdimensional invertible map (p=2, 3)," Int. J. Bifurcation and Chaos 13, 1787-1810.

[21] C. Mira, and L. Gardini, (2009), "From the box-withina-box bifurcation organization to the Julia set. Part I: Revisited properties of the sets generated by a quadratic complex map with a real parameter," Int. J. Bifurcation and Chaos 19, 281–327.

[22] C. Mira, (2013), "Embedding of a Dim1 piecewise continuous and linear Leonov map into a Dim2 invertible map," "Global Analysis of Dynamic Models in Economics and Finance," eds. G. I. Bischi, et al. (Springer, Berlin, Heidelberg), pp. 337-367.

[23] H. Li, K. Li, M. Chen and B. Bao, (2020), "Coexisting infinite orbits in an area-preserving Lozi map," Entropy 22, 1119.

[24] F. Tramontana and L. Gardini, (2021), "Revisiting Samuelson's models, linear and nonlinear, stability conditions and oscillating dynamics," Tramontana and Gardini Economic Structures 10:9 https://doi.org/10.1186/s40008-021-00239-3, Journal of Economic Structures.

[25] M. Misiurewicz, and S. Stimac, (2016), "Symbolic dynamics for Lozi maps," Nonlinearity 29, 3031

[26] D. Simpson, (2014), "Sequences of periodic solutions and infinitely many coexisting attractors in the bordercollision normal form," Int. J. Bifurcation and Chaos 24, 1430018-1-18.

[27] I. Sushko V. Avrutin and L. Gardini, (2021), "Center Bifurcation in the Lozi Map," International Journal of Bifurcation and Chaos, Vol. 31, No. 16 2130046 (28 pages), World Scientific Publishing Company DOI: 10.1142/S0218127421300469.